RSC Advances

ROYAL SOCIETY OF CHEMISTRY

www.rsc.org/advances

Cite this: DOI: 10.1039/c0xx00000x

www.rsc.org/xxxxxx

ARTICLE TYPE

Understanding of Thiol-Induced Etching of Luminescent Gold Nanoclusters

*Chen-Yi Ke[a], Tzu-Heng Chen[a], Lin-Chen Lu[a], and Wei-Lung Tseng[a,b,c]**

Received (in XXX, XXX) Xth XXXXXXXXX 20XX, Accepted Xth XXXXXXXXX 20XX

DOI: 10.1039/b000000x

This study reported that lysozyme Type VI (Lys VI)-stabilized Au_8 clusters serve as a model to probe how distinct types of alkanethiol ligands affect the core etching of AuNCs. By monitoring the fluorescence of Au_8 clusters, we determined that thioglycolic acid (TGA)-induced core etching of Au_8 clusters was substantially faster at pH 9.0 than it was at pH 3.0. This can be attributed to more efficient electron injection from TGA to Au_8 clusters at pH 9.0, facilitating the core etching of Au_8 clusters. Because long-chain mercaptoalkanoic acids attached to Au_8 clusters are considerably disordered and exhibit a high density of gauche defects, the ability of mercaptoalkanoic acid to etch Au_8 clusters increased when the alkyl chain length was decreased. The thiol analogs exhibited the following trend in the core etching of Au_8 clusters at pH 9.0: TGA > 2-mercaptoethanol > 1-octanethiol. These results indicate that the carboxyl group of ligand is a key element for the core etching of Au_8 clusters. We also disclosed that Au_8 clusters can protect Lys VI activity against denaturation and act as a fluorescent probe to detect thimerosal in vaccines.

1 Introduction

The thiol functional group is a key component in numerous chemical and biological agents that exhibit potent reactivity and biological activities (e.g., reduction of protein disulfides). [1] Thiol groups are used as building blocks in numerous chemical reactions, including organic synthesis (e.g., alkylations, Michael additions, and cross-coupling reactions) and the labeling of biomolecules (e.g, click chemistry and thioglycosides-related reaction).[2, 3] Since the late 1980s, substantial research has examined preparing self-assembled monolayers (SAMs) of thiols on bulk gold surfaces by forming robust Au-S bonds with energies in the range of 30–40 kcal/mol.[4] Based on SAM chemistry, thiols have been widely used to modify and stabilize gold nanoparticles (AuNPs), thiol-stabilized AuNPs have been proven suitable for use in the fields of sensors,[5] catalysts,[6] nanomedicine,[7] and molecular imaging.[8]

Recently, diverse methods have been used to prepare gold nanoclusters (AuNCs) that emit fluorescence from the near-IR to UV regions in the presence of thiols. These AuNCs not only exhibit ultrasmall size, long fluorescent lifetimes, size-tunable emission wavelengths, high catalytic properties, and photo-stability,[9] but also act as fluorescent probes to compete with quantum dots and fluorescent proteins. The synthesis of the AuNCs with thiols are classified into four types: (1) direct reduction of gold precursor to AuNCs in the presence of thiol,[10, 11] (2) thermodynamic selection for the synthesis of the most stable AuNCs after size focusing of a mixture of different sized AuNCs with thiol,[12] (3) conversion of small-sized cluster to large-sized one by performing ligand exchange with thiol-containing ligands (e.g., Au_{11} to Au_{25} and Au_{55} to Au_{75}),[13, 14] and (4) thiol-induced core etching of large-sized gold nanoparticles (AuNPs) to AuNCs.[15-17] For example, the size-focusing methodology has been successfully established to generate molecularly pure Au_{25}, Au_{38}, or Au_{144} clusters in the presence of thiols. Thiols can selectively crash unstable AuNCs and permit the most stable AuNCs to survive.[12] In addition to the size-focusing method, Chang and coworkers prepared green-emitting AuNCs by reducing a gold precursor to AuNPs with tetrakis(hydroxyl-methyl)phosphonium chloride (THPC), and etching the generated AuNPs with 11-mercaptoundecanoic acid.[15] Using a similar methodology, Chang and coworkers also reported the synthesis of α-d-mannose-conjugated AuNCs by replacing THPC with thiol-modified mannose.[16] Pradeep and coworkers reported that both glutathione (GSH) and bovine serum albumin (BSA) (that included one free cysteine residue) could etch mercaptosuccinic acid-capped AuNPs to produce AuNCs.[17, 18] Arakawa and coworkers determined that Au_5 and Au_8 clusters were produced as a result of the pepsin-triggered core etching of Au_{13} clusters.[19] Among these synthetic methods, the thiol-induced core-etching approach can be used to effectively generate fluorescent AuNCs and precisely control the size of these AuNCs at the atomic level. To understand the role of thiols in the etching process, we explored the detailed reaction mechanism is crucial. However, studies published to date have not clearly explained the thiol-induced core-etching process.

In this study, attaching various alkanethiol ligands onto the surface of Lysozyme Type VI (Lys VI)-stabilized Au_8 clusters regulated the etching rate between ligands and AuNCs. The alkyl chain length and the functional groups of ligands were

[a] *Department of Chemistry, National Sun Yat-sen University, Kaohsiung, Taiwan. Fax: 011-886-7-3684046; E-mail: tsengwl@mail.nsysu.edu.tw*

[b] *School of Pharmacy, College of Pharmacy, Kaohsiung Medical University, Taiwan.*

[c] *Center for Nanoscience and Nanotechnology, National Sun Yat-Sen University, 70, Lien-Hai Road, Kaohsiung 80424, Taiwan*

Ke, C.-Y. and Chen, T.-H. contributed equally to the work

† Electronic Supplementary Information (ESI) available: Fig. S1-S10. See DOI: 10.1039/b000000x/

determined to be major factors governing the thiol-induced core etching of AuNCs. Furthermore, our results reveal that blue-emitting Au_8 clusters can be used to detect thimerosal in vaccines and that the thiol-induced etching of Au_8 clusters can be used to regulate lysozyme activity.

2 Methods

Chemical

Hydrogen tetrachloroaurate (III) dehydrate was purchased from Alfa-Aesar (Ward Hill, MD, USA). Na_2HPO_4, NaH_2PO_4, TGA, 3-mercaptopropanoic acid 6-mercaptohexanoic acid, 8-mercaptooctanoic acid, 2-mercaptoethanol, 1-octanethiol, GSH, thimerosal, EtHg, 2,2'-dithiosalicylic acid, TSA, metal ions, and anions were ordered from Sigma-Aldrich (St. Louis, MO, USA). PC_2, PC_3, and PC_4 were purchased from AnaSpec (San Jose, CA, USA). Lys VI (from chicken egg white), BSA (from bovine serum), and ovalbumin (from chicken egg white) was ordered from MP Biomedicals (Irvine, CA). Milli-Q ultrapure water (Milli-Pore, Hamburg, Germany) was used in all of the experiments.

Apparatus

The absorption and fluorescence spectra of AuNCs were collected using a double-beam UV-vis spectrophotometer (Cintra 10e; GBC, Victoria, Australia) and a Hitachi F-7000 fluorometer (Hitachi, Tokyo, Japan), respectively. The elemental compositions of Lys VI-stabilized Au_8 clusters were measured by JAMP-9500F Auger Electron Spectroscopy (JEOL, Japan). Circular dichroism experiments were conducted using a JASCO model J-810 circular dichroism spectropolarimeter (JASCO Corporation, Tokyo, Japan). Environmental scanning electron microscopy (FEI Quanta 200 FEG, Holand FEI Company) was used for the observation of the Au^+-TGA coordination polymer. The molecular weight of Lys VI-stabilized Au_8 clusters were measured using an Autoflex I matrix-assisted laser desorption/ionization time-of-flight mass spectrometry (MALDI-TOF MS; Bruker Daltonics, Germany) equipped with a nitrogen UV laser (337 nm wavelength, 3 ns laser pulse duration). Prior to MALDI-TOF MS measurements, saturated α-cyano-4-hydroxycinnamic acid containing 70% acetonitrile was mixed with an equal volume of Lys VI-stabilized Au_8 clusters. The resulting mixtures were pipetted onto a stainless steel 384-well target (Bruker Daltonics, Germany) and dried in air. Inductively-coupled plasma MS (Perkin-Elmer-SCIEX, Thornhill, ON, Canada) was used to measure the Au content in the supernatant, which is obtained from the centrifugation of a solution containing 125 μM TGA and Au_8 clusters.

Synthesis of Protein-Stabilized AuNCs

The synthesis of protein-stabilized AuNCs was according to the previous procedure.[20-22] A solution of 25 mg mL^{-1} Lys VI reacted with an equal volume of 10 mM $HAuCl_4$ at 37 °C for 12 h. The pH of the resulting solutions was adjusted to pH 3.0 and 12.0 to obtain Lys VI-stabilized Au_8 and Au_{25} clusters, respectively. For preparing BSA- and ovalbumin-stabilized Au_8 clusters, a solution of $HAuCl_4$ (5 mL, 10 mM) was mixed with protein (5 mL, 20 mg mL^{-1}) under vigorous stirring. After that, ascorbic acid (50 μL, 0.35 mg mL^{-1}) was added to the resulting solution and incubated them at 37°C for 12 h.

Etching of AuNCs by Thiol

A solution of protein-stabilized Au_8 clusters (50 μL) was incubated with thiol (950 μL, 125 μM) in 10 mM phosphate buffer (pH 3.0 and 9.0) at ambient temperature for 10 min. After centrifugation of the resulting solution at 175000 rpm (34230 g force) for 3 min, the obtained supernatant was transferred into a 1 mL quartz cuvette. Their fluorescence spectra were recorded by operating the fluorescence spectrophotometer at an excitation wavelength of 380 nm. The precipitate was purified by washing twice with distilled water. XPS and SEM were used to analyze the purified precipitate.

Fluorescence Assay of Thiomersal

All chemicals were prepared in 5 mM phosphate buffer (pH 3.0). Thiomersal (900 μL, 0.6-100 μM) was incubated with Lys VI-stabilized Au_8 clusters at ambient temperature for 0-20 min. After centrifugation of the resulting solution at 17500 rpm (34230 g force) for 3 min, we transferred the obtained supernatant into a 1 mL quartz cuvette and measured their fluorescence spectra at an excitation wavelength of 380 nm. To test the selectivity of Lys VI-stabilized Au_8 clusters, thimerosal was replaced by 2,2'-dithiosalicylic acid (900 μL 100 μM), EtHg (900 μL 100 μM), TSA (900 μL, 100 μM), metal ions (900 μL, 100 μM), and anions (900 μL, 100 μM), one at a time. For sensing thimerosal in vaccine, 2 mL of tetanus vaccine was centrifuged at 107500 rpm for 20 min to remove alumina gel. The supernatant solutions (1.9 mL) were diluted to 10-fold with 5 mM phosphate buffer (pH 3.0). We spiked the resulting solutions (800 μL) with standard thimerosal (100 μL, 1-80 μM) and incubated them with Lys VI-stabilized Au_8 clusters (100 μL) at ambient temperature for 20 min. The following steps were the same as those used in the sensing of thimerosal in 5 mM phosphate buffer.

Measurement of Lys VI activity

A solution of Lys VI-stabilized AuNCs was dialyzed with 5 mM phosphate buffer (pH 3.0) for one day. The purified AuNCs (100 μL) and Lys VI were separately incubated with GSH (900 μL, 0-10 mM) at ambient temperature for 10 min. The mixture was diluted to 20-fold with 1X reaction buffer (pH 7.5) containing 0.1 M sodium phosphate, 0.1 M NaCl, and 2 mM sodium azide. Levels of Lys VI activity in the resulting solution was determined using the EnzChek Lysozyme assay kit (E-22013; Molecular Probes, Eugene, OR).

3 Results and Discussion

3.1 Effect of functional groups and alkyl chain length of alkanethiols on the etching of Au_8 clusters

The details of the methods used to synthesize AuNCs are described in the experimental section. Briefly, blue-emitting, Lys VI-stabilized Au_8 clusters were prepared by mixing Lys VI

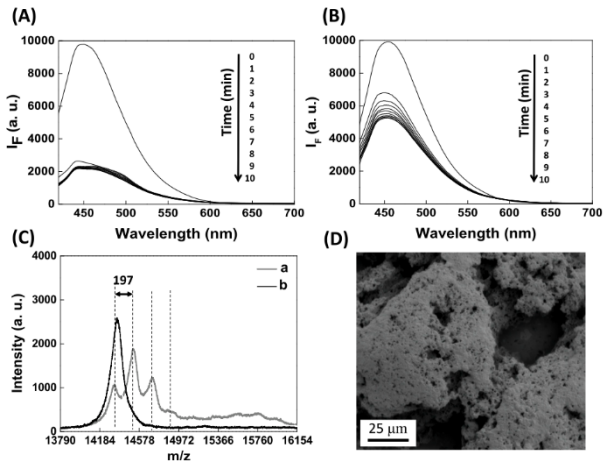

Figure 1. Time-dependent fluorescence spectra of Lys VI-stabilized Au_8 clusters upon the addition of 125 μM TGA at (A) pH 9.0 and (B) pH 3.0. (C) MALDI-TOF mass spectra of Lys VI-stabilized Au8 cluster in the (a) absence and (b) presence of 125 μM TGA. (D) SEM image of the precipitate obtained from centrifugation of a mixture of Lys VI-stabilized Au_8 clusters and TGA. The incubation time between protein-stabilized Au_8 clusters and TGA is (A, B) 0-10 and (C, D) 10 min.

with $HAuCl_4$ at pH 3.0 and stirring at 37 °C for 12 h. Upon excitation at 380 nm, previous study have demonstrate that the strong emission at 455 nm originated from Lys VI-stabilized Au_8 clusters, rather than from the native fluorescence of Lys VI.[20] Note that cysteine residues of Lys VI can stabilize Au_8 clusters due to the strong interaction between Au and thiol groups.[23] Because the fluorescence intensity of Au_8 clusters is highly responsive to the concentration of GSH,[20] we monitored the fluorescence spectra of Au_8 clusters in the presence of a series of mercaptoalkanoic acids. Figures 1A and 1B show the time-dependent fluorescence spectra obtained for Au_8 clusters that were incubated with thioglycolic acid (TGA) at pH 9.0 and 3.0, respectively. We note that Au_8 clusters converted to Au_{25} clusters upon exposure to 12.0.[20] This conversion did not occurred at pH 9.0. The TGA-induced core etching of Au_8 clusters was completed in 2 min at pH 9.0, whereas this reaction was slow at pH 3.0. TGA-induced core etching of Au_8 clusters arose from electron injection from TGA to Au_8 clusters.[24-26] This electron injection can create an electric stress on Au_8 clusters, making them electronically unstable. To relieve this stress, Au_8 clusters undergoes size-reduction *via* the coulomb explosion of surface charges. At pH 9.0, the thiol group of TGA can quickly attach onto the surface of Au_8 clusters, resulting in more efficient electron injection from TGA to Au_8 clusters. Thus, at pH 9.0, the addition of TGA to a solution of Au_8 clusters caused a sudden decay in their fluorescence. In comparison, at pH 3.0, slow attachment of TGA onto the surface of Au_8 clusters causes less efficient electron transfer between them. Thus, the TGA-induced core-etching reaction of Au_8 clusters was markedly slow at pH 3.0, resulting in a gradual decrease in the fluorescence of Au_8 clusters. Figure 1A displays that a shallow bump developing around 450–500 nm was observed with time. This is probably attributed to the increase of the formation of Au^+-TGA coordination polymers with time.[27]

To confirm that the fluorescence signal decreased because of TGA-induced core etching of Au_8 clusters, we measured the fluorescence spectra at various concentrations of TGA. The fluorescence intensity of Au_8 clusters at 455 nm decreased linearly with increasing the concentration of TGA from 0 to 120 mM (Figure S1, ESI). Because MALDI-TOF-MS can be used to determine the presence of Au_n clusters,[19, 20, 28, 29] we performed MALDI-TOF-MS to prove TGA-induced etching of Au_8 clusters at pH 9.0. The MALDI-TOF-MS spectrum obtained for Lys VI-stabilized Au_8 clusters displayed multiple peaks between *m*/*z* 14000 and 15000 corresponding to a series of fragments of Lys VI-stabilized Au_8 clusters (curve a in Figure 1C). The peaks appearing at *m*/*z* 14322, 14519, 14716, and 14913 (with Au spacing), were assigned to $[Lys\ VI]^+$, $[Lys\ VI + Au]^+$, $[Lys\ VI + Au_2]^+$, and $[Lys\ VI + Au_3]^+$, respectively. However, the peak corresponding to $[Lys\ VI + Au_8]^+$ was not observed because high laser power could induce the production of fragmentation of Lys VI-stabilized Au_8 clusters under gas-phase condition. Similarly, Kawasaki et al. found that the MALDI-TOF-MS spectrum of pepsin-mediated Au_8 clusters consisted of Au_5, Au_6 and Au_7 clusters.[19] By contrast, the peaks corresponding to $[Lys\ VI + Au_n]^+$ clusters could not be detected after incubating Au_8 clusters with TGA at pH 9.0 (curve b in Figure 1C). Furthermore, when Au_8 clusters were incubated with 125 μM TGA, the mixture became cloudy and insoluble products were generated.[27] Scanning electron microscopy images clearly showed that the resulting products exhibited a porous structure, which likely arose from the aurophilic Au^+–Au^+ interaction-facilitated formation of Au^+-TGA coordination polymers (Figure 1D). Similarly, Shen et al. indicated that a mixture of Ag^+ and cysteine converted into a coordination polymer as a result of the argentophilic Ag^+–Ag^+ interaction and the electrostatic interactions among the side chains in the polymeric backbone.[30] The elemental composition of the insoluble products was determined using X-ray photoelectron spectroscopy (XPS). The XPS spectrum of the insoluble products exhibited peaks at 162.7 eV (Au-S bond) and 168.0 eV (S-O bond), confirming the formation of the Au-S bonds and the oxidation of thiols (Figure S2, ESI). Next, we used inductively coupled plasma MS to measure the Au content of the supernatant obtained after removing the insoluble products by centrifuging the samples. When 125 μM TGA was added to a solution of Au_8 clusters, the Au concentrations in the supernatants sharply decreased at 2 min, reaching reached a plateau after 2 additional min (Figure S3, ESI). This result largely agrees with the observation that the fluorescence of Au_8 clusters decreased sharply in the presence of TGA at pH 9.0. Collectively, these findings demonstrate that TGA etched the Au_8 clusters into an Au^+-TGA coordination polymer.

To examine whether the chain length of mercaptoalkanoic acid affected the thiol-induced core etching of Au_8 clusters. Measuring the fluorescence after incubating the samples for 10 min indicated that the fluorescence intensity of Au_8 clusters at 455 nm gradually decreased when the chain length of

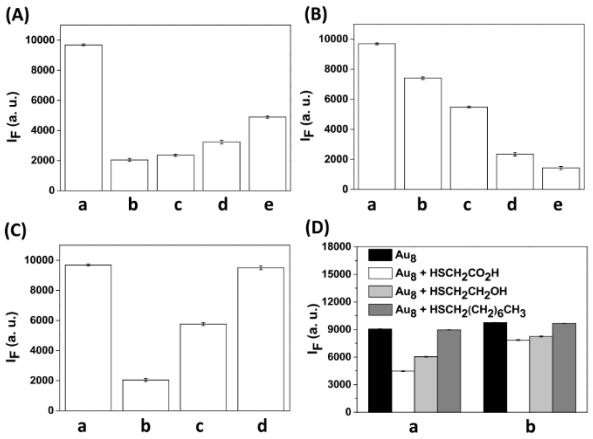

(Figure 2A). These results indicate that short-chain

Figure 2. (A-C) Fluorescence intensity at 455 nm of Lys VI-stabilized Au8 clusters after adding (A) mercaptoalkanoic acids, (B) thiol-containing peptides, and (C) thiol-containing ligands. (D) Fluorescence intensity at 405 nm of BSA-stabilized AuNCs and at 430 nm of ovalbumin-stabilized AuNCs after adding TGA, 2-mercaptoethanol, and 1-octanethiol. (A): (a) Au_8, (b) Au_8 and TGA, (c) Au_8 and 3-mercaptopropanoic acid, (d) Au_8 and 6-mercaptohexanoic acid, and (e) Au_8 and 8-mercaptooctanoic acid. (B): (a) Au_8, (b) Au_8 and GSH, (c) Au_8 and PC_2, (d) Au_8 and PC_3, and (e) Au_8 and PC_4. (C): (a) (a) Au_8, (b) Au_8 and TGA, (c) Au_8 and 2-mercaptoethanol, and (d) Au_8 and 1-octanethiol. (D): (a) BSA-stabilized AuNCs and (b) ovalbumin-stabilized AuNCs. The incubation time between protein-stabilized AuNCs and ligands is 10 min. The concentration of each thiol is 125 μM. The excitation wavelengths are 330, 375, and 380 nm for BSA-, ovalbumin-, and Lys VI-stabilized Au_8 clusters, respectively.

mercaptoalkanoic acid was increased from 2 to 7 carbon atoms mercaptoalkanoic acid etched Au_8 clusters more rapidly than did the long-chain form of the acid. Because an increase in the alkyl chain length causes an increase in its title angle,[31] gauche defects and entropic contributions are postulated to become increasingly critical in mercaptoalkanoic acids featuring a long carbon chain.[32] These findings imply that long-chain mercaptoalkanoic acids attached on the Au surface are likely to be substantially disordered, exhibiting a high density of gauche defects. Thus, the number of ligand molecules attached per Au_8 cluster increased as the length of the alkyl chain of mercaptoalkanoic acid decreased. Similarly, Hinterwirth et al. determined that the number of mercapto-alkanoic acid molecules attached per AuNP diminished when the chain length of the acid was increased.[33] Collectively, these findings indicate that when the number of ligand molecules attached to Au_8 clusters is increased, the electron injection from ligand molecules to Au_8 clusters is strengthened, facilitating the core etching of Au_8 clusters.

To further confirm the above-mentioned result, thiol-containing peptides including GSH and phytochelatins were incubated with Au_8 clusters for 10 min at ambient temperature. The general structure of phytochelatins is (γ-glutamate-cysteine)$_n$–glycine (PC_n). Our results (Figure 2B) indicated the

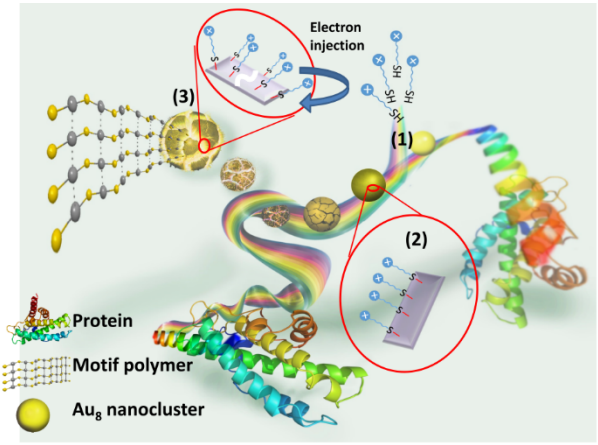

Figure 3. Schematic illustration for thiol-induced core etching of protein-stabilized Au_8 clusters.

fluorescence intensity of Au_8 clusters at 455 nm gradually decreased when the number of γ-glutamylcysteine units per molecule was increased. Previous studies have reported that the thiol group of ligand was determined to be a major factor governing the etching of AuNPs.[24-26] Thus, an increase in the number of the thiol groups of ligand molecules causes more efficient electron injection from ligand molecules to Au_8 clusters; this effect was amplified by increasing the number of γ-glutamylcysteine units from 2 to 4 in phytochelatin.

The relation between the type of functional group present on the thiol-containing ligand and the core etching of Au_8 clusters is presented in Figure 2C. Compared with incubating with TGA, incubating Au_8 clusters with 2-mercaptoethanol resulted in a smaller reduction in the fluorescence intensity of Au_8 clusters at 455 nm, indicating that the core etching of Au_8 clusters induced by TGA was faster than was that induced by 2-mercaptoethanol. Previous studies have disclosed that the carboxyl groups of ligand molecules attached on the surface of AuNPs were capable of interacting with free ligand molecules *via* the formation of hydrogen bonding, leading to more efficient electron injection.[24-26] Thus, compared to 2-mercaptoethanol, TGA attached on the surface of Au_8 clusters facilitates to bring free TGA to approach the surface of Au_8 clusters $_{via}$ intermolecular hydrogen bonding, resulting in more efficient electron injection from TGA (free and attached TGA) to Au_8 clusters

To determine that the carboxyl group of ligand is a key element for ligand-induce core etching of Au_8 clusters, a neutral ligand, 1-octanethiol, was selected in the following study. In the presence of 1-octanethiol, the fluorescence of Au_8 clusters at 455 nm remained almost constant, suggesting that 1-octanethiol could not etch Au_8 clusters because the attached 1-octanethiol was incapable of interacting with free 1-octanethiol *via* the formation of hydrogen bonding. These results indicate that a small change in the terminal group of ligand is sufficient for dominating the rate of thiol-induced etching of Au_8 clusters. To demonstrate that the etching mechanism described here can be

extended to other protein-stabilized Au_8 clusters, we replaced Lys VI with either BSA or ovalbumin. When excited at 380 nm, the fluorescence maxima of BSA- and ovalbumin-stabilized AuNCs were centered, respectively, at approximately 405 and 430 nm (Figure S4, ESI), suggesting that the size of the 2 AuNCs formed could be similar to that of Au_8 clusters *via* the spherical Jellium model.[34] The emission wavelengths were nearly equal to those reported for Au_8 clusters stabilized with polyethylenimine (λ_{em} = 455 nm),[35] BSA (λ_{em} = 450 nm),[36] and Lys VI (λ_{em} = 455 nm).[20] The results in Figure 2D demonstrate that the etching rate depended on the degree of dissociation of the functional group of the thiol-containing ligand in both BSA- and ovalbumin-stabilized AuNCs. Similarly, 11-mercaptoundecanoic acid was demonstrated to be more efficient than 2-mercaptoethanol and 6-mercaptohexanol were at etching THPC-capped AuNPs.[15] Based on these results and those of previous studies, we conclude that 3 parts of a thiol molecule are involved in the electron injection-induced core etching of Au_8 clusters (Figure 3): (1) the sulfur headgroups, which are linked to the surface of Au_8 clusters as a result of the formation of strong Au-S bonds; (2) the hydrocarbon chains of neighboring thiol molecules, which produce an ordered monolayer on the surface of Au_8 clusters; and (3) the terminal groups of thiol molecules, which interacts with free ligands *via* the formation of hydrogen bonding.

3.2 Lys VI-stabilized Au_8 clusters for Sensing Thimerosal

Thimerosal, which consists of thiosalicylic acid (TSA) and the ethylmercuric (EtHg) ion, is widely used as antimicrobial preservative in vaccines and cosmetics.[37] Because thimerosal is metabolized to TSA and EtHg in the human body, thimerosal-containing vaccines have been suggested to cause neurodevelopmental disorders.[38] To assess the health risk that thimerosal poses, a rapid, convenient, and sensitive method is required to routinely analyze thimerosal dosage in pharmaceutical products. Because carboxylic group-containing thiols can efficiently etch Au_8 clusters, we hypothesized that the TSA-induced fluorescence quenching of Lys VI-stabilized Au_8 clusters occurred after the decomposition of thimerosal into TSA and EtHg (Figure 4A). Curve a in Figure S5 (ESI) reveals that Au_8 clusters exhibited strong fluorescence at 455 nm when present in a solution of 5 mM sodium phosphate at pH 3.0, indicating that Lys VI can stabilize Au_8 clusters at low pH. The fluorescence spectrum of Au_8 clusters remained unchanged in the presence of 100 μM EtHg (Curve b in Figure S5, ESI). By contrast, adding either 100 μM TSA or 100 μM thimerosal to a solution of Au_8 clusters caused a fluorescence decrease at 455 nm, indicating that TSA and thimerosal etched Au_8 clusters (Curves c and d in Figure S5, ESI). Thus, we attributed thimerosal-induced core etching of Au_8 clusters to the presence of TSA, rather than to the presence of EtHg. Figure S6 (ESI) reveals that the thimerosal-induced etching of Au_8 clusters was nearly complete in 20 min. However, Reader et al. previously reported that 0.001% thimerosal was completely decomposed into TSA and EtHg in water after 8 days.[39] Thus, the rapid etching observed here can be attributed to the ability of AuNCs

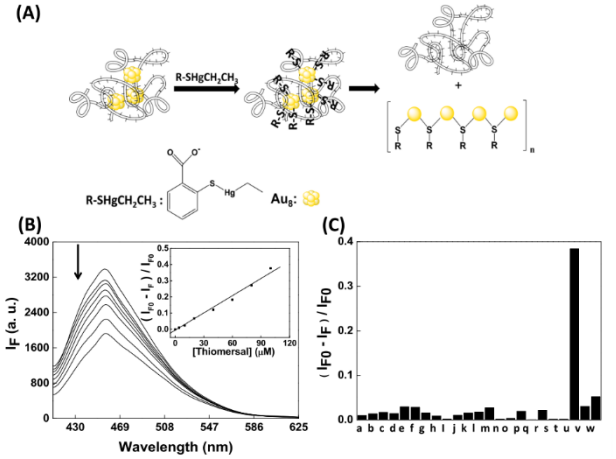

Figure 4. (A) Description of fluorescence detection of thimerosal based on TSA-induced core etching of Lys VI-stabilized Au_8 clusters. (B) Fluorescence spectra of Lys VI-stabilized Au_8 clusters in the presence of 0-100 μM thimerosal. Inset: a plot of the $(I_{F0}-I_F)/I_{F0}$ value at 455 nm versus the thimerosal concentration. The arrow indicates the signal changes with increases in analyte concentration (0, 4, 10, 20, 40, 60, 80, and 100 μM). The error bars represent standard deviations based on three independent measurements. (C) The $(I_{F0}-I_F)/I_{F0}$ value at 455 nm of Lys VI-stabilized Au_8 clusters after the addition of (a) Na^+, (b) K^+, (c) Ba^{2+}, (d) Cr^{3+}, (e) Mn^{2+}, (f) Fe^{2+}, (g) Fe^{3+}, (h) Pb^{2+}, (i) Ag^+, (j) Cd^{2+}, (k) Hg^{2+}, (l) Li^+, (m) Mg^{2+}, (n) Ca^{2+}, (o) Sr^{2+}, (p) Co^{2+}, (q) Cu^{2+}, (r) Zn^{2+}, (s) Au^{3+}, (t) NH^{4+}, (u) thimerosal, (v) EtHg, and (w) 2,2'-dithiosalicylic acid. The concentration of each analyte is 100 μM. (C, D) The incubation time is 20 min.

to catalyze the decomposition of thimerosal through the formation of Au-thiolate on the surface of AuNCs. A similar phenomenon was observed in the case of AuNP-catalyzed decomposition of *S*-nitrosoglutathione.[40] When the concentration of thimerosal was increased, the fluorescence spectra of Au_8 clusters showed a gradual reduction in the fluorescence at 455 nm (Figure 4B), and a clear linear relationship was observed between the value of $(I_{F0}-I_F)/I_{F0}$ and thimerosal concentration in the range of 4–100 μM (R^2 = 0.9865; inset in Figure 4B). I_{F0} and I_F represent the fluorescence intensities of the Au_8 clusters at 455 nm in the absence and presence of added thimerosal, respectively. At a signal-to-noise ratio of 3, the limit of detection measured for thimerosal was 1 μM, which is considerably lower compared with the level of thimerosal used in vaccines (0.003% to 0.01%).[38] Next, we evaluated the thimerosal selectivity of Au_8 clusters. Figures 4C and S7 (ESI) indicate that the $(I_{F0}-I_F)/I_{F0}$ values of Au_8 clusters changed within 20 min after separately adding metal ions, 2,2'-dithiosalicylic acid, and anions. Adding only thimerosal and iodide was sufficient to cause a clear change in the $(I_{F0}-I_F)/I_{F0}$ value, whereas adding EtHg and 2,2'-dithiosalicylic acid induced a negligible change in the $(I_{F0}-I_F)/I_{F0}$ value, indicating that the

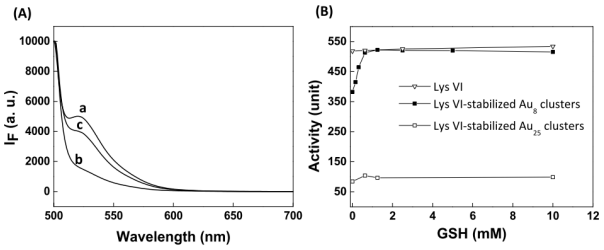

Figure 5. (A) Fluorescence spectra of fluorescein obtained from the use of EnzChek Lysozyme Assay Kit for measuring the activity of (a) Lys VI, (b) Lys VI-stabilized Au_{25} clusters, and (c) Lys VI-stabilized Au_8 clusters. (B) Effect of the concentration of GSH on the activity of Lys VI, Lys VI-stabilized Au_{25} clusters, and Lys VI-stabilized Au_8 clusters. The final concentration of Lys VI is 0.03 mg/mL. The incubation time between the AuNCs and GSH is 10 min.

probe developed here exhibits high selectively toward thiol-containing compounds. Because iodide can react with AuNPs to form AuI_2^- complexes, the fluorescence of Au_8 clusters decreased when iodide was added. Thus, we suggest that Lys VI-stabilized Au_8 clusters can be used as an effective fluorescent-sensor of iodide.

Our results demonstrated the feasibility of using Au_8 clusters to detect thimerosal in vaccines. The value of $(I_{F0} - I_F)/I_{F0}$ decreased after 10-fold-diluted vaccine samples were spiked with standard solutions containing various concentrations of thimerosal (Figure S8, ESI). The slope of the calibration curve obtained from the spiked sample resembled that obtained from the standard samples, indicating that the matrix effect of the vaccine sample did not measurably influence the probe. By using the external calibration curve, the concentration of thimerosal in the vaccine sample was estimated to be 250 ± 30 μM; this value agrees with the listed thimerosal concentration of the vaccine.

3.3 Au_8 clusters efficiently control Lys VI activity

Immobilizing enzymes on AuNPs has been suggested to modulate the catalytic properties of the enzymes by altering their substrate-binding affinity, accelerating product formation, and enhancing enzyme stability.[41-43] Therefore, we investigated how Au_8 clusters influenced the activity of Lys VI, which we measured using the fluorescence-based EnzChek Lysozyme Assay Kit. This assay is based on the lysozyme-mediated hydrolysis of *Micrococcus lysodeikticus* cells, which releases fluorescein conjugated to the cells. Comparing the fluorescence spectra of fluorescein-conjugated cells incubated with Lys VI (Curve a in Figure 5A) and Lys VI attached to Au_{25} clusters (Curve b) shows that the attachment of the Au_{25} clusters completely inhibited the activity of Lys VI. By contrast, following attachment to Au_8 clusters, Lys VI activity was inhibited by approximately 30% (Curve c in Figure 5A). This result indicates that the AuNCs can suppress the activity of Lys VI. Figure 5B indicates that the activity of Lys VI-stabilized Au_8 clusters gradually increased with the addition of 0 to 1.3 mM GSH, reaching saturation at the GSH concentration of 2.5 mM; the fluorescence spectra corresponding to these samples are shown in Figure S9 (ESI). These results demonstrate that GSH can etch the Au_8 clusters, thereby restoring the activity of Lys VI, signifying that the activity of Lys VI can be efficiently regulated by varying the concentration of GSH. By contrast, the activity of Lys VI-stabilized Au_{25} clusters remained low and unchanged in the presence of increasing concentrations of GSH. This is because the Au_{25} clusters consist of an Au_{13} core and 6 [–S–Au–S–Au–S–] oligomers and therefore inhibit GSH-induced etching of the AuNCs.[44] Because the intracellular GSH concentration (1—10 mM) and extracellular thiol levels differ substantially, we suggest that Lys VI, which serves as a protein-drug model, can be activated by intracellular GSH.

We also examined the stability of Lys VI and Lys VI-stabilized Au_8 clusters by incubating them at pH 2.0 for 12 h, after which the solutions were adjusted to pH 7.5 and the enzyme activity was measured using the EnzChek Lysozyme Assay Kit. Following incubation, both the Lys VI-stabilized Au_8 clusters and Lys VI lost 30% of their initial activity (Figure S10, ESI). However, when Lys VI-stabilized Au_8 clusters and Lys VI were separately mixed with a solution of 2.5 mM GSH, only the activity of Lys VI-stabilized clusters was restored to 100% of the initial activity. These results suggest that Au_8 clusters can stabilize Lys VI by protecting the enzyme against denaturation.

Conclusions

We used Lys VI-stabilized Au_8 clusters as a model to probe how the length and the functional groups of thiol ligands affect thiol-induced core etching of protein-stabilized AuNCs. Our results indicate that the core etching of AuNCs increases when (1) the thiol groups of ligand molecules is increased, (2) the chain length of the ligand is decreased, and (3) the carboxyl group of ligand molecule is present. These observations elucidate the mechanism of the thiol-induced core etching of protein-stabilized AuNCs: First, thiol molecules rapidly attach to the AuNC surface through the formation of Au-S bond. Second, excess thiol molecules attach to the AuNC surface and the number of ligand molecules on the AuNC surface decreases as the ligand chain length increases. Third, the AuNCs are etched to Au^+-thiol coordination polymers as a result of the electron injection from ligand molecules to Au_8 clusters. Short-chain mercaptoalkanoic acid can etch Au_8 clusters, and because of this property, the Au_8 clusters can be used to detect thimerosal in vaccines. Furthermore, the core etching of AuNCs by GSH in a concentration-dependent manner allows GSH to be used to regulate the activity of Lys VI-stabilized Au_8 clusters.

Acknowledgements

We would like to thank the National Science Council (NSC 100-2628-M-110-001-MY4) for the financial support of this study.

Notes and references

1. C. E. Paulsen and K. S. Carroll, *Chem. Rev.*, 2013, **113**, 4633-4679.
2. M. H. Stenzel, *ACS Macro Lett.*, 2013, **2**, 14-18.
3. C. X. Yin, F. J. Huo, J. J. Zhang, R. Martinez-Manez, Y. T. Yang, H. G. Lv and S. D. Li, *Chem. Soc. Rev.*, 2013, **42**, 6032-6059.
4. C. D. Bain and G. M. Whitesides, *Angew. Chem. Int. Edit.*, 1989, **28**, 506-512.

5. K. Saha, S. S. Agasti, C. Kim, X. Li and V. M. Rotello, *Chem. Rev.*, 2012, **112**, 2739-2779.
6. M. C. Daniel and D. Astruc, *Chem. Rev.*, 2004, **104**, 293-346.
7. R. Arvizo, R. Bhattacharya and P. Mukherjee, *Expert opinion on drug delivery*, 2010, **7**, 753-763.
8. J. Gao, X. Huang, H. Liu, F. Zan and J. Ren, *Langmuir*, 2012, **28**, 4464-4471.
9. Y. Lu and W. Chen, *Chem. Soc. Rev.*, 2012, **41**, 3594-3623.
10. Y. Negishi, K. Nobusada and T. Tsukuda, *J. Am. Chem. Soc.*, 2005, **127**, 5261-5270.
11. H. Yang, Y. Wang and N. Zheng, *Nanoscale*, 2013, **5**, 2674-2677.
12. R. C. Jin, H. F. Qian, Z. K. Wu, Y. Zhu, M. Z. Zhu, A. Mohanty and N. Garg, *J. Phys. Chem. Lett.*, 2010, **1**, 2903-2910.
13. Y. Shichibu, Y. Negishi, T. Tsukuda and T. Teranishi, *J. Am. Chem. Soc.*, 2005, **127**, 13464-13465.
14. R. Balasubramanian, R. Guo, A. J. Mills and R. W. Murray, *J. Am. Chem. Soc.*, 2005, **127**, 8126-8132.
15. C.-C. Huang, Z. Yang, K.-H. Lee and H.-T. Chang, *Angew. Chem. Int. Edit.*, 2007, **46**, 6824-6828.
16. C.-C. Huang, Y.-L. Hung, Y.-C. Shiang, T.-Y. Lin, Y.-S. Lin, C.-T. Chen and H.-T. Chang, *Chem. Asian J.*, 2010, **5**, 334-341.
17. M. A. Habeeb Muhammed, P. K. Verma, S. K. Pal, A. Retnakumari, M. Koyakutty, S. Nair and T. Pradeep, *Chem. Eur. J.*, 2010, **16**, 10103-10112.
18. M. Habeeb Muhammed, S. Ramesh, S. Sinha, S. Pal and T. Pradeep, *Nano Res.*, 2008, **1**, 333-340.
19. H. Kawasaki, K. Hamaguchi, I. Osaka and R. Arakawa, *Adv. Funct. Mater.*, 2011, **21**, 3508-3515.
20. T. H. Chen and W. L. Tseng, *Small*, 2012, **8**, 1912-1919.
21. Y.-H. Lin and W.-L. Tseng, *Anal. Chem.*, 2010, **82**, 9194-9200.
22. T. Das, P. Ghosh, M. S. Shanavas, A. Maity, S. Mondal and P. Purkayastha, *Nanoscale*, 2012, **4**, 6018-6024.
23. Y. L. Xu, J. Sherwood, Y. Qin, D. Crowley, M. Bonizzoni and Y. P. Bao, *Nanoscale*, 2014, **6**, 1515-1524.
24. T. Wang, X. G. Hu and S. J. Dong, *Chem Commun*, 2008, 4625-4627.
25. S. Riaz, L. L. Qu, E. K. Fodjo, W. Ma and Y. T. Long, *Rsc Adv*, 2014, **4**, 14031-14034.
26. S. Riaz, W. Ma, C. Jing, M. H. Nawaz, D. W. Li and Y. T. Long, *Chem Commun*, 2013, **49**, 1738-1740.
27. Y. Shichibu, Y. Negishi, H. Tsunoyama, M. Kanehara, T. Teranishi and T. Tsukuda, *Small*, 2007, **3**, 835-839.
28. J. Xie, Y. Zheng and J. Y. Ying, *J. Am. Chem. Soc.*, 2009, **131**, 888-889.
29. A. Dass, A. Stevenson, G. R. Dubay, J. B. Tracy and R. W. Murray, *J. Am. Chem. Soc.*, 2008, **130**, 5940-5946.
30. J. S. Shen, D. H. Li, M. B. Zhang, J. Zhou, H. Zhang and Y. B. Jiang, *Langmuir*, 2011, **27**, 481-486.
31. L. Ramin and A. Jabbarzadeh, *Langmuir*, 2011, **27**, 9748-9759.
32. F. Schreiber, *Prog. Surf. Sci.*, 2000, **65**, 151-257.
33. H. Hinterwirth, S. Kappel, T. Waitz, T. Prohaska, W. Lindner and M. Lammerhofer, *ACS Nano*, 2013, **7**, 1129-1136.
34. J. Zheng, P. R. Nicovich and R. M. Dickson, *Annu. Rev. Phys. Chem.*, 2007, **58**, 409-431.
35. H. Duan and S. Nie, *J. Am. Chem. Soc.*, 2007, **129**, 2412-2413.
36. X. Le Guevel, B. Hotzer, G. Jung, K. Hollemeyer, V. Trouillet and M. Schneider, *J. Phys. Chem. C*, 2011, **115**, 10955-10963.
37. S. Trumpler, W. Lohmann, B. Meermann, W. Buscher, M. Sperling and U. Karst, *Metallomics*, 2009, **1**, 87-91.
38. L. K. Ball, R. Ball and R. D. Pratt, *Pediatrics*, 2001, **107**, 1147-1154.
39. M. J. Reader and C. B. Lines, *Journal of pharmaceutical sciences*, 1983, **72**, 1406-1409.
40. H. Y. Jia, Y. Liu, X. J. Zhang, L. Han, L. B. Du, Q. Tian and Y. C. Xu, *J. Am. Chem. Soc.*, 2009, **131**, 40-41.
41. C. S. Wu, C. T. Wu, Y. S. Yang and F. H. Ko, *Chem. Commun.*, 2008, 5327-5329.
42. J. Deka, A. Paul and A. Chattopadhyay, *RSC Adv.*, 2012, **2**, 4736-4745.
43. Y. C. Shiang, C. C. Huang, T. H. Wang, C. W. Chien and H. T. Chang, *Adv. Funct. Mater.*, 2010, **20**, 3175-3182.
44. M. Zhu, C. M. Aikens, F. J. Hollander, G. C. Schatz and R. Jin, *J. Am. Chem. Soc.*, 2008, **130**, 5883-5885.